Horiyama *et al. Journal of Wood Science* (2023) 69:37
https://doi.org/10.1186/s10086-023-02112-2

Journal of Wood Science

NOTE

Transition in viscoelastic properties within successive annual rings of radiata pine (*Pinus radiata*)

Hiroaki Horiyama[1], Keisuke Kojiro[1*] and Yuzo Furuta[1]

Abstract

Dynamic mechanical analysis (DMA) measurements of water-saturated radiata pine wood in the temperature range from 0 ℃ to 100 ℃ were focused to clarify the transition in viscoelastic properties within successive annual rings. Four radially consecutive specimens were taken per annual ring and DMA measurements in the tangential direction were performed using these specimens. The following results were obtained. The peak of tanδ caused by micro-Brownian motion of lignin was observed in all samples. The temperature of peak tanδ tended to decrease from earlywood to latewood within an annual ring. The temperature of peak tanδ increased across annual ring boundary. The same trend was repeated within the next annual ring. It was found that the viscoelastic properties transitioned within successive annual rings.

Introduction

Wood is a metabolic product of trees, which are living organisms, and its properties are much more diverse than those of industrially produced materials. Tree growth is a complex phenomenon. Wood density, annual ring width, and the proportion of latewood (LW) to earlywood (EW) are influenced by local climate, environmental pollution, and silvicultural practices [e.g., 1–3]. Annual ring structure, especially EW and LW, in conifers have been the subject of numerous studies [4–7]. The wall thickness of LW is greater than that of EW, and the diameter of the lumen of LW is smaller than that of EW. Therefore, the density of LW is considered to be greater than that of EW and appears darker in color. The differences in physical properties within annual ring are mostly explained by differences in density, or cell wall thickness [8]. On the other hand, it has been reported that lignin concentration varies with site within an annual ring [9–11]. Saka and Thomas reported the distribution of lignin in the cell walls of EW and LW of Loblolly pine by bromination using the SEM-EDXA system [10]. The lignin concentration in EW is 0.20 g/g in the S2 layer and 0.49 g/g in the composite middle layer (CML), while in LW it is 0.18 g/g in the S2 layer and 0.51 g/g in the CML [10]. Instead of using visible annual rings, some studies have used alternative indicators, such as stable carbon ($\delta^{13}C$) and oxygen isotope ratios ($\delta^{18}O$) of wood, which change with the seasons [12–16]. Kagawa et al. reported the results of pulse-labeling whole trees to determine how photosynthates in spring, summer and autumn are used in the formation of both EW and LW [15]. Analysis of intra-annual $\delta^{13}C$ of the tree rings formed after the labeling revealed that EW contained photosynthates from the previous year's summer and autumn as well as from the current spring, while LW was mainly composed of photosynthates from the current year's summer and autumn, although it also relied on stored material in some cases [15]. There are numerous reports describing wood characteristics in terms of anatomical and chemical characteristics within annual ring. On the other hand, there are

*Correspondence:
Keisuke Kojiro
kojiro@kpu.ac.jp
[1] Graduate School of Life and Environmental Sciences, Kyoto Prefectural University, Kyoto 606-8522, Japan

few reports expressing wood properties in terms of variation in physical properties within annual rings.

In this study, we focused on radiata pine which has a wide range of annual rings to understand the transitions in physical properties within the annual rings in more detail. Radiata pine is also a commercial species, and there have been various reports on it for a long time [17–21]. Biblis reported that specific gravity increases from EW to LW within a growth ring, with a corresponding increase in tensile strength and modulus of elasticity (MOE) [22]. However, our previous studies have reported that differences in physical properties within an annual ring cannot be explained solely by differences in density [23]. We also focused on the dynamic mechanical analysis (DMA), a method that can measure the viscoelastic properties of wood. Viscoelastic properties of wood have been used to understand the structure of wood at the molecular level, because they strongly reflect the effect of the structural state of wood components [23–27]. For example, it has been reported those the thermal softening behavior of water-saturated wood changes when the structure of lignin in the cell wall changes [25]. Our previous studies have shown that the thermal softening properties of EW and LW of Douglas fir are different, with a peak of tanδ at about 95 °C for EW and 90 °C for LW [23]. Peak temperatures of tanδ have also been shown to be lower for LW than for EW in other softwoods [24]. In addition, viscoelastic properties are a very important parameter in the industrial use of wood [28]. Understanding the transition in viscoelastic properties within successive annual rings is of great importance in terms of understanding trees biologically and their industrial use. Therefore, DMA measurements were performed in the tangential direction on successive sections of water saturated radiata pine wood to clarify the transition in viscoelastic properties within successive annual rings.

Materials and methods

Materials

The samples used for measurements were radiata pine (*Pinus radiata*). In this study, samples were cut from two consecutive annual rings in a one block. The sample sizes were 1.2 mm in the radial direction (R), 30 mm in the tangential direction (T), and 1.0 mm in the longitudinal direction (L) for the measurement of dynamic viscoelastic properties. The schematic diagram of samples is shown in Fig. 1. The samples were boiled for 2 h in distilled water and then annealed to room temperature in those to make them saturated.

Scanning electron microscope (SEM)

The cross section of the samples was planned using a sliding microtome. The samples were dried at 105 °C for 24 h, and then the cross section was observed using SEM

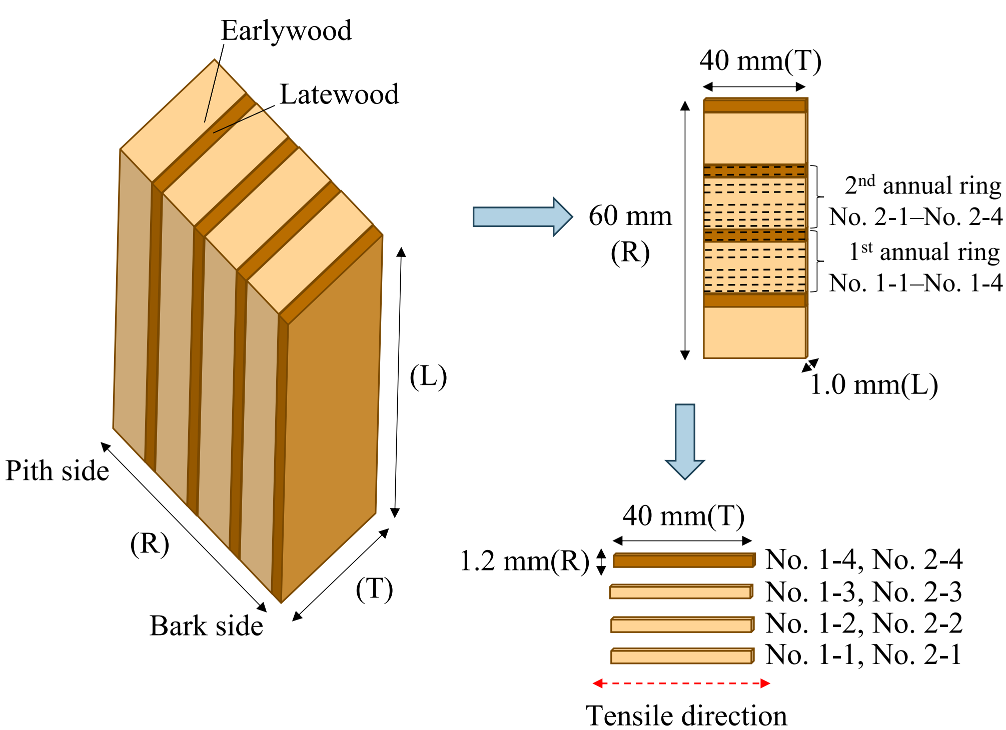

Fig. 1 Schematic diagram of sample shape of dynamic mechanical analysis (DMA)

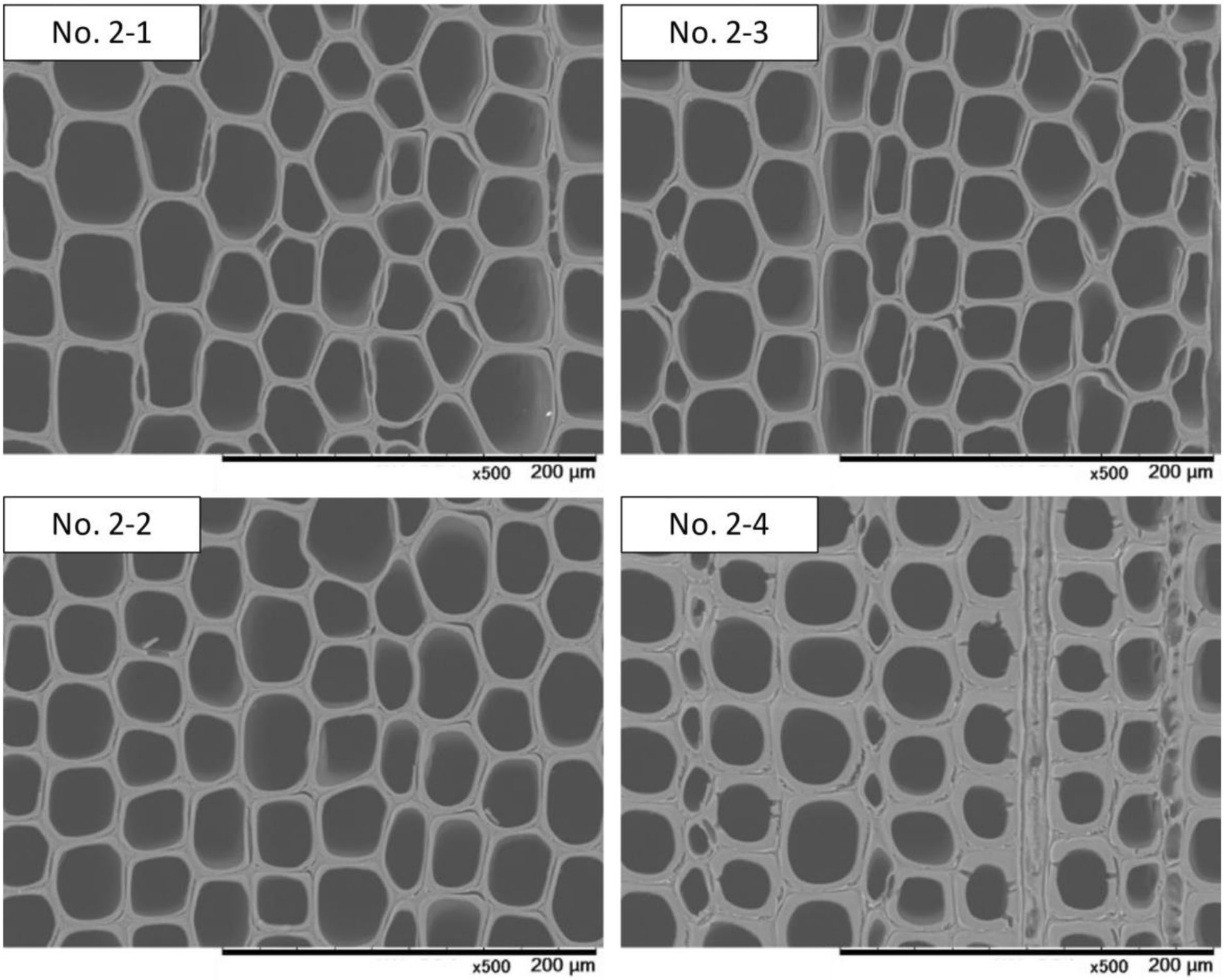

Fig. 2 SEM images of radiata pine wood within 2nd annual ring used in this study

(TM3030 Plus Miniscope, Hitachi High-Technologies, Tokyo, Japan) at an accelerating voltage of 15 kV. Software ImageJ (National Institutes of Health, USA) was used to measure the cell wall thickness. As for the cell wall thickness, it is the thickness between the cell wall and lumen boundary of two adjacent parenchyma cells or two fiber cells. The distance between the lumens (thickness of two cell walls) of two tracheids was measured, and half of this value was used as the cell wall thickness of the tracheid. The distance was measured at a total of 50 points on the tangential and radial walls, respectively.

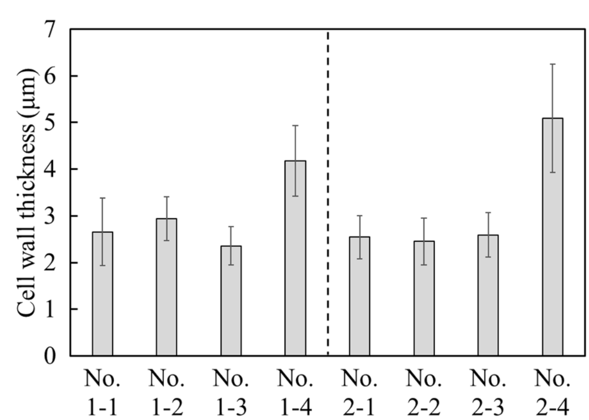

Fig. 3 Cell wall thickness of radiata pine wood within each annual ring. Error bars are standard deviations. The dashed line in the figure is the annual ring boundary

Dynamic mechanical analysis (DMA)

Temperature dependence of storage modulus (E'), loss modulus (E''), and tanδ were measured by the tensile forced oscillation method using a dynamic mechanical

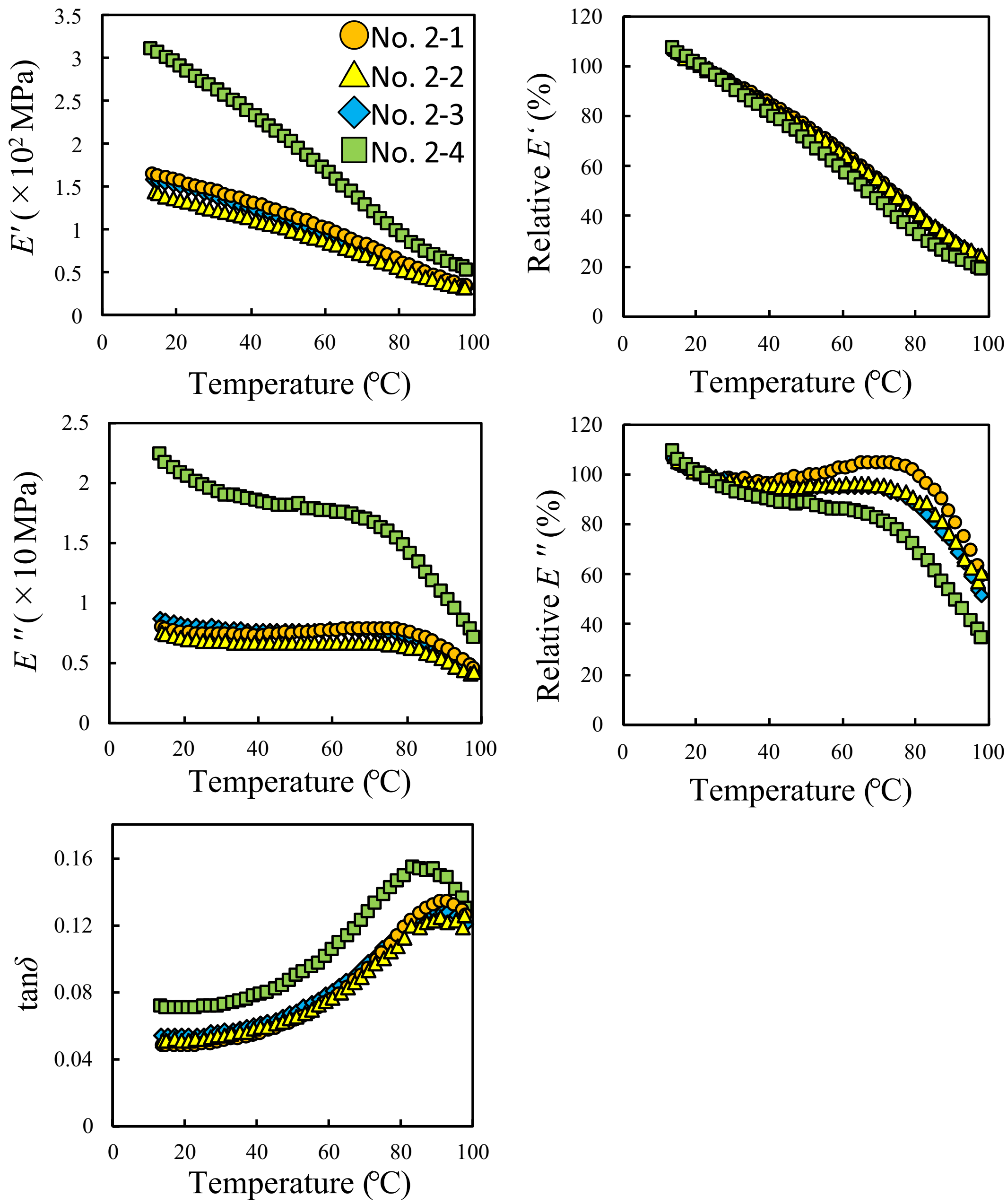

Fig. 4 Temperature dependence of E', E'', tanδ, relative E' and relative E'' within 2nd annual ring of radiata pine swollen by water at 0.5 Hz. Measurement direction was tangential direction. Relative E' and relative E'' are relative to values at 20 ℃

analyzer (DMS6100, Seiko Instruments, Chiba, Japan). The samples swollen by the distilled water were measured in the distilled water at a temperature range of 20 ℃ to 95 ℃. The heating and cooling rate was 1 ℃/min. Frequencies for the measurement were 0.5, 1.0, 2.0, 5.0, and 10 Hz. The span was 12 mm, and the displacement amplitude was 5 µm. The tensile direction was tangential. Results were obtained in the second heating process to uniform the heating and cooling histories [25].

Results and discussion

Figure 2 shows SEM images for the cross section of radiata pine used in this study, indicating that the sample is normal wood, neither reaction wood nor starved wood. Nos. 1-1–1-4 were omitted due to the same trend as Nos. 2-1 –2-4. As shown in Fig. 3, the thickness of the cell walls ranged from about 2.5 µm to 5.0 µm. Walmsley et al. reported average wall thicknesses of 2.87 µm,

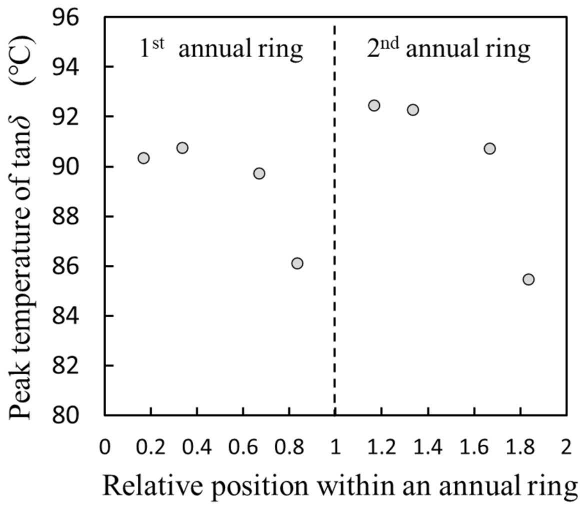

Fig. 5 Peak temperatures of tanδ for radiata pine wood within each annual ring. Relative positions are standardized with each annual ring width as 1. The dashed line in the figure is the annual ring boundary

3.38 μm, 4.64 μm, and 4.79 μm for inner EW, outer EW, inner LW, and outer LW of radiata pine, respectively, which is consistent with the results of this study [29].

Figure 4 shows the temperature dependence of E', E'', tanδ, relative E' and relative E'' within 2nd annual ring of radiata pine swollen by water at 0.5 Hz. Nos. 1-1–1-4 were omitted due to the same trend as Nos. 2-1 –2-4. E' of all the measured EW and LW decreased with increasing temperature in the range of 20 ℃ to 100 ℃. E'' of No. 2-1 within an annual ring increased from 20 ℃ to 80 ℃ and then decreased to 100 ℃. Those of No. 2-4 decreased slightly from 20 ℃ to 60 ℃ and then rapidly decreased to 100 ℃. Those of Nos. 2-2 and 2-3 within an annual ring slightly decreased from 20 ℃ to 40 ℃, then leveled off, followed by a gradual decreased from 80 ℃ to 100 ℃. The peaks of tanδ were found at around 90 ℃ for EW and around 85 ℃ for LW Those peaks, which appear in the range of 0 ℃ to 100 ℃, are attributed to the micro-Brownian motion of lignin [25]. E', E'', and tanδ of LW were higher than these of EW in each temperature. In general, the differences in various mechanical properties between EW and LW are considered to be largely due to density. It has been reported that there is a correlation between the absolute value of E' and density [30]. In the previous report, when E' and E'' of Douglas-fir EW and LW are divided by density, the values at each temperature are close [23]. However, it has been reported that differences in thermal softening behavior cannot be explained by differences in density alone [23]. The decrease in relative E' with increasing temperature was found to be greater for No. 2-4 than for No. 2-1. There was no difference in relative E' within Nos. 2-1–2-3. As for relative E'', it was found to vary widely within the annual ring. In the No. 2-1, there was a significant increase in relative E'' with increasing temperature from 40 ℃ to 80 ℃, but this increase was less pronounced in the Nos. 2-2 –2-3, and not in the No. 2-4. In general, the reason for the increase in relative E'' is that the cohesive structure of molecular chains is gradually released as the glass transition begins, and the strain on the object due to external forces tend to increase, resulting in an increase in the energy lost due to strain. The rightward slope after reaching the relative E'' peak is due to the fact that the total energy associated with strain, which had been decreasing, since the glass transition began, becomes smaller as the entanglement of molecular chains dissolves to some extent. This is because the loss energy also becomes smaller in dependence on it. The peak temperatures of tanδ plotted in relative position in the annual ring are shown in Fig. 5. Relative positions are standardized with each annual ring width as 1. A trend of decreasing peak temperature of tanδ was obtained from No. 1-1 or No. 2-1 to No. 1-4 or No. 2-4, respectively. In addition, the peak temperature was found to increase when crossing the annual ring boundary from No. 1-4 to No. 2-1. The results of this study indicate that there is transition in thermal softening behavior within successive annual rings. In other words, it is very likely that components, especially matrix components, such as lignin, differ depending on the site within an annual ring. In the future, we would like to clarify the relationship between the amount and molecular state of the components and the thermal softening properties.

Conclusions

To understand the transition in viscoelastic properties within successive annual rings, four radially consecutive specimens were taken per annual ring from water-saturated radiata pine wood and DMA measurements in the tangential direction were performed using these specimens. A decreasing trend in temperature of peak tanδ was obtained within an annual ring from EW to LW. An increase in peak temperature was observed across the annual ring boundary. The same trend was repeated within the next annual ring. These results clarified that the viscoelastic properties transit within successive annual rings.

Abbreviations

LW	Latewood
EW	Earlywood
R	Radial direction
T	Tangential direction
L	Longitudinal direction
DMA	Dynamic mechanical analysis
E'	Storage modulus

E'' Loss modulus
SEM Scanning electron microscope
EDX Energy dispersive X-ray spectroscopy
CML Composite middle layer
MOE Modulus of elasticity

Acknowledgements
Not applicable.

Author contributions
HH designed the study, collected and analyzed data and wrote the initial draft of the manuscript. KK and YF contributed to dynamic viscoelastic analysis and interpretation of data. All authors agree to be accountable for all aspects of the work in ensuring that questions related to the accuracy or integrity of any part of the work are appropriately investigated and resolved. All authors read and approved the final manuscript.

Funding
Not applicable.

Availability of data and materials
The data sets generated during and/or analyzed during the current study are available from the corresponding author on reasonable request.

Declarations

Ethics approval and consent to participate
Not applicable.

Consent for publication
Not applicable.

Competing interests
The authors declare that they have no competing interests.

Received: 4 August 2023 Accepted: 17 November 2023
Published online: 03 December 2023

References
1. Baas P, Bauch J (Eds.) (1986) The effects of environmental pollution on wood structure and quality. Rijksherbarium for the International Association of Wood Anatomists
2. Schweingruber FH (2012) Tree rings: basics and applications of dendrochronology. Springer Science & Business Media, Cham
3. Polge H (1978) Fifteen years of wood radiation densitometry. Wood Sci Technol 12:187–196
4. Saiki H (1963) Studies on the annual ring structure of coniferous wood. II. Demarcation between earlywood and latewood (1). Mokuzai Gakkaishi 9(6):231–236
5. Saiki H (1963) Studies on the annual ring structure of coniferous wood. III. Demarcation between earlywood and latewood. Mokuzai Gakkaishi. 9(6):237–243
6. Saiki H (1965) Studies on the annual ring structure of coniferous wood. IV. Effects of diameter decrease and cellwall thickning of tracheid on latewood formation. Mokuzai Gakkaishi. 11(1):1–6
7. Saiki H (1965) Studies on the annual ring structure of coniferous wood. V. Variation from the pith toward outside. Mokuzai Gakkaishi. 11(5):185–190
8. Büyüksarı Ü, As N, Dündar T (2017) Mechanical properties of earlywood and latewood sections of Scots pine wood. BioResources 12(2):4004–4012
9. Fergus BJ, Procter AR, Scott JAN, Goring DAI (1969) The distribution of lignin in sprucewood as determined by ultraviolet microscopy. Wood Sci Technol 3(2):117–138
10. Saka S, Thomas RJ (1982) A study of lignification in loblolly pine tracheids by the SEM-EDXA technique. Wood Sci Technol 16(3):167–179
11. Saka S, Goring DAI (1988) The distribution of lignin in white birch wood as determined by bromination with TEM-EDXA 42:149-153
12. Leavitt SW, Long A (1991) Seasonal stable-carbon isotope variability in tree rings: possible paleoenvironmental signals. Chem Geol Isot Geosci Sect 87:59–70
13. Evans MN, Schrag DP (2004) A stable isotope-based approach to tropical dendroclimatology. Geochim Cosmochim Acta 68:3295–3305
14. Poussart PF, Evans MN, Schrag DP (2004) Resolving seasonality in tropical trees: multi-decade, high-resolution oxygen and carbon isotope records from Indonesia and Thailand. Earth Planet Sci Lett 218:301–316
15. Kagawa A, Sugimoto A, Maximov TC (2006) $^{13}CO_2$ pulse-labelling of photoassimilates reveals carbon allocation within and between tree rings. Plant, Cell Environ 29(8):1571–1584
16. Ohashi S, Durgante FM, Kagawa A, Kajimoto T, Trumbore SE, Xu X, Ishizuka M, Higuchi N (2016) Seasonal variations in the stable oxygen isotope ratio of wood cellulose reveal annual rings of trees in a Central Amazon terra firme forest. Oecologia 180:685–696
17. Donaldson LA (1985) Within- and between-tree variation in lignin concentration in the tracheid cell wall of *Pinus radiata*. NZ J Forest Sci 15(3):361–369
18. Donaldson LA (1991) Seasonal changes in lignin distribution during tracheid development in *Pinus radiata* D. Don Wood Sci Technol 25:15–24
19. Donaldson LA (1992) Lignin distribution during latewood formation in *Pinus radiata* D. Don IAWA J 13(4):381–387
20. Donaldson L, Xu P (2005) Microfibril orientation across the secondary cell wall of Radiata pine tracheids. Trees 19:644–653
21. Sharma M, Brennan M, Chauhan SS, Entwistle KM, Altaner CM, Harris PJ (2015) Wood quality assessment of *Pinus radiata* (radiata pine) saplings by dynamic mechanical analysis. Wood Sci Technol 49:1239–1250
22. Biblis EJ (1969) Transitional variation and relationships among properties within loblolly pine growth rings. Wood Sci Technol 3:14–24
23. Horiyama H, Kojiro K, Okahisa Y, Imai T, Itoh T, Furuta Y (2022) Combined analysis of microstructures within an annual ring of Douglas fir (*Pseudotsuga menziesii*) by dynamic mechanical analysis and small angle X-ray scattering. J Wood Sci 68(1):52
24. Horiyama H, Miyoshi Y, Kojiro K, Furuta Y (2023) Thermal softening properties of various wood species within an annual ring. J Wood Sci 69:30
25. Furuta Y, Nakajima M, Nakatani T, Kojiro K, Ishimaru Y (2008) Effects of lignin on the thermal-softening properties of water-swollen wood. J Soc Mater Sci Japan 57(4):344–349
26. Furuta Y, Masamitsu N, Nakanii E, Ohkoshi M (2010) The effects of lignin and hemicellulose on thermal-softening properties of water-swollen wood. Mokuzai Gakkaishi 56(3):132–138
27. Kojiro K, Miki T, Sugimoto H, Nakajima M, Kanayama K (2010) Micropores and mesopores in the cell wall of dry wood. J Wood Sci 56:107–111
28. Seki M, Yashima Y, Abe M, Miki T, Nishida M (2022) Influence of delignification on plastic flow deformation of wood. Cellulose 29(7):4153–4165
29. Walmsley MRW, Hodgson KT, O'reilly T, Kibblewhite RP, Lloyd J, Richardson J (2007) Physical and chemical properties of earlywood and latewood radiata pine and Douglas fir kraft fibres. Appita Technol Innov Manuf Environ. 60(3):209–216
30. Brémaud I, Ruelle J, Thibaut A, Thibaut B (2013) Changes in viscoelastic vibrational properties between compression and normal wood: roles of microfibril angle and of lignin. Holzforschung 67(1):75–85